Thermal Cycling Damage of High Temperature Metal Matrix Composites

TATSUO MORIMOTO* and MINORU TAYA
Department of Mechanical Engineering, FU–10, University of Washington, Seattle, Washington 98195, USA

* on leave from Mitsubishi Heavy Industries, Ltd., Advanced Technology Research Center, 1-8-1 Sachiura, Kanazawa-ku, Yokohama, Japan

ABSTRACT

Thermal cycling damage of two different types of superalloy metal matrix composite, namely tungsten continuous fiber/FeCrAlY composite and FP alumina short fiber/FeCrAlY composite, were studied experimentally, the effectiveness of short fibers in reducing the thermal cycling damage was also discussed.

KEYWORDS

Metal matrix composites; thermal cycling damage; high temperature composite; superalloy; FP alumina/FeCrAlY composite; W-ThO_2/FeCrAlY composite; thermal expansion

INTRODUCTION

Metal matrix composite (MMC) is considered to be a strong candidate as structural material for high temperature applications such as gas turbine and engine components. Among the severe requirements for the high temperature material, thermal fatigue resistance is considered to be one of the most important properties. Many studies on this subject have been made; tungsten/copper (Yoda, *et al.*, 1979), SiC/titanium (Park and Marcus, 1983), boron/aluminum (Chawla, 1976; Olsen and Tompkins, 1979), FP alumina/magnesium (Bhatt and Grimes, 1983), tungsten/FeCrAlY (Petrasek and Signorelli, 1981) and SiC whisker/aluminum (Patterson and Taya, 1985; Taya and Mori, 1987). These studies have revealed that the mismatch of thermal expansion coefficient (CTE) between fiber and matrix is the main driving force in causing the internal debonding or excess plastic deformation in the metal matrix, thus resulting in the degradation of the macroscopic properties and dimensional change of MMC. The summary of degradation of MMCs due to thermal cycling has recently been given in a book by Taya and Arsenault (1989). Minimizing CTE mismatch will improve thermal cycling resistance of composite. Therefore, one of the successful ways to reduce the CTE mismatch is to add another filler (modifier) which will make the average CTE of the matrix phase smaller, thus reducing the mismatch (note that the CTE of fiber is quite small compared with that of matrix). The advantage of this method is to reduce the thermal stress at the interface between continuous fiber and matrix. Jackson *et al.* (1987) reported the reduction of the CTE of FeCrAlY (CTE = 20×10^{-6}/°C) by adding alumina powder (CTE = 8×10^{-6}/°C). With the above concept of using the modifier phase to improve the thermal cycling resistance of selected MMC systems in mind, we are conducting a series of experiments. This paper will report some of the preliminary results i.e., CTE measured and thermal cycling damage of two types of FeCrAlY based MMC.

First we will describe materials and experiment, and then the experimental results, followed by discussion. Finally a conclusion is given.

MATERIALS AND EXPERIMENT

Material

FeCrAlY alloy powder (325 mesh average size.) provided by Union Carbide Co., Indianapolis, Indiana was used for matrix material. A chemical composition of FeCrAlY powder is given elsewhere (Petrasek and Signorelli, 1981). Two types of reinforcement were used; FP alumina chopped (or short) fiber of 1.7×10^{-2}mm in diameter, 2mm in average length, and W-1%ThO_2 continuous fiber of 0.2mm in diameter. FP alumina fiber was provided by E.I. du Pont de Nemours and Co., Wilmington, Delaware in the form of a continuous fiber tape with a fugitive binder. W-1%ThO_2 fiber was provided by General Electric Company, Cleveland, Ohio.

Composite Processing Route.

FP alumina Fiber/FeCrAlY. FP alumina chopped fiber and FeCrAlY powder were mixed so that fiber could be dispersed uniformly. Fiber volume fraction (V_f) was aimed at 5% and 15%. The mixture was filled in a steel container shown in Fig.1, then sealed and evacuated. Then the container was consolidated by HIP (hot isostatic press) with 152MPa at 1473K. HIP process was done by Boeing Aerospace Co., Renton, Washington.

W-ThO_2fiber/FeCrAlY. FeCrAlY powder was blended with molten paraphine and was made into thin plate of 1mm in thickness. W-ThO_2 fibers were cut from bundles, aligned and fixed with fugitive tape, then laid up with matrix plate into steel container one by one. After the binder had been removed from both fiber mat and matrix plate by heating, the container was sealed with the same procedure described above, then HIP processed. Fiber volume fraction (V_f) was aimed at 9%. A schematic diagram of composite processing route is shown in Fig.2 and Table 1 indicates an outline of the composite specimens.

Table 1. Composite Specimen

Type of Fiber	Fiber Volume Fraction (V_f) %	Matrix	Name of Composite
Chopped FP Alumina	5	FeCrA1Y	5% V_f Fp Alumina Composite
Chopped FP Alumina	15	FeCrA1Y	15% V_f Fp Alumina Composite
Continuous W-ThO_2	9	FeCrA1Y	W-ThO_2 Composite
none	0	FeCrA1Y	Unrreinforced Matrix

Experiment

Thermal Expansion. The coefficient of thermal expansion (CTE) of each sample of cylindrical shape (13mm in length, 8mm in diameter) was measured by formaster over the temperature range from room temperature up to 1373°K.

Thermal Cycling Tests. MMC of cylindrical shape samples (70mm in length, 10mm in diameter) were thermal cycled by the thermal cycling testing apparatus of the University of Washington, which consists of two different furnaces and transportation units, and the specimen was shuttled between two furnaces with a preset time interval (Armstrong and Taya, 1988). In this experiment, the maximum temperature ($T_{max.}$) was set at 1373 K and minimum temperature ($T_{min.}$) was set at room temperature, and the duration for each cycle was 12 minutes, namely 6 minutes stay in each furnace. A typical temperature-time curve is shown in Fig.3. After

thermal cycling, the residual tensile properties of cycled specimens and also those of uncycled specimens were measured by tensile tests where the tensile test specimen is of dog-bone type with 25.4mm in gauge length and 6.35mm in diameter. The microstructure of these specimens were observed by scanning electron microscope (SEM) with the aim of detecting the debonding at the interface between fibers and matrix.

EXPERIMENTAL RESULTS

Microstructure of As-Processed MMC Specimens

W-ThO_2 composite. A typical microstructure of the cross section of as-processed W-ThO_2 composite is shown in Fig.4. Due to the thickness of initial powder plate and small V_f, there exists some unevenness in fiber distribution, but no debonding or crack was observed.

FP alumina composite. Extensive observations were made on as-processed FP alumina composites with the aim of assessing the orientation of FP alumina short fibers. To this end, we have cut out a number of cubes with their surface revealing X-, Y- and Z-surfaces (referred to X, Y, Z cordinates to Fig. 1). The SEM observations on these surfaces have led us to conclude that short fibers are distributed almost randomly in a three-dimensional space. Short fibers were then extracted from these cubes and used to generate the distribution of fiber aspect ratio (l/d). The average value of l/d, $\overline{l/d}$ was calculated as 123.24.

Thermal Expansion

Figures. 5 and 6 show the results of the thermal expansions of FP alumina/FeCrAlY and W-ThO_2/FeCrAlY composites, respectively. It is seen clearly from Fig. 5 that for a given temperature the thermal expansion decreases with increase in the volume fraction of fiber V_f and also it increases with temperature T. This non-linear temperature dependence is due to the non-linear temperature dependence of the thermal expansion of the matrix since the thermal expansion of fiber (α -Al_2O_3 fiber) is linear on T, i.e. constant CTE over T. Unlike FP alumina composite system, the thermal expansion behavior of W-ThO_2 continuous fiber composite appears to consist of two stages as seen in Fig. 6; the first stage being non-linear temperature dependent (its slope, i.e., CTE increases with T) and the second stage with the smaller CTE. In this composite system, the temperature dependence of thermal expansion of W-ThO_2 fiber is slightly non-linear, i.e., CTE increases slightly with T

Thermal Cycling

Dimensional Change. Figure. 7 shows the several specimens (matrix, W-ThO_2 composite and FP alumina composites) before and after thermal cycling 100 and 200 times. In each photo, the top and the lower photos denote uncycled and cycled MMC specimens, respectively. It follows from Fig. 7 that W-ThO_2 composite specimen exhibited relatively large warping, which was attributed to non-uniform distribution of W-ThO_2 fibers (Fig. 4), while in FP alumina composites only small amount of warping was observed. Figures. 8 and 9 indicate the relative dimensional change along the radial and axial directions of the thermally cycled specimens. It is seen from Fig. 8 that in FP alumina composites the positive dimensional change along both directions was observed although its amount is small, whereas W-ThO_2 composite exhibited the swelling along the radial direction at the cost of the shrinkage along the radial direction (i.e., perpendicular to W-ThO_2 fibers). It is noted in Figs. 7 and 9 that the dimensional change of the 100 times cycled W-ThO_2 composite along the axial direction is considered to be overestimated due to the excess warping (Fig. 7), thus the filled square symbol at N = 100 should move toward upward, resulting in smoother change of the axial dimensional change over N.

Microstructure Change. Extensive scanning electron microscopy (SEM) study was conducted with the aim of finding some evidence of the dimensional changes observed in the cycled MMC specimens. However, no apparent damage due to thermal cycling was observed in both 5% and 15%V_f FP alumina composites. This may be due to the small size of such damage in this composite system if any exists. On the other hand, in W-

ThO_2 composite specimen, some microcracks were observed, and the density of the microcracks are higher in the cycled specimen (Fig. 10 (b)) than in the uncycled specimen (Fig.10 (a)).

Tensile Properties. The thermally cycled MMC and unreinforced matrix specimens were subjected to tensile tests to obtain the residual tensile properties. The data on the strength of the cycled MMC specimens are given as a function of number of thermal cycles in Fig. 11 where the data of the uncycled specimens are also shown. It is noted from Fig. 11 that 5%V_f FP alumina composite exhibits the best mechanical performance in both uncycled and cycled conditions among three MMCs while the strength of W-ThO_2 composite is slightly larger than that of the unreinforced matrix. It is also noted in Fig. 11 that the strength of 15%V_f FP alumina composite decreases rapidly with number of thermal cycle as well as its uncycled strength is lower than that of 5%V_f FP alumina composite.

DISCUSSION

CTE of Composites. Coefficient of Thermal Expansion (CTE) of MMCs can be calculated from the slopes of the thermal expansion-temperature curves of Fig. 5 (FP alumina composite) and Fig. 6 (W-ThO_2 composite). Since CTE is not constant over the temperature range tested, piecewise CTE is calculated for each 100 K interval, and the results are compared with the Levin's lower bound (α_L) (Levin, 1967) and shown in Table 2

Table 2. Thermal expansion coefficient of composites.

Temp.*** Range	Matrix	W-ThO_2 Fiber	9% V_f ThO_2 Composite		5% V_f FP Composite		15% V_f FP Composite	
	Experiment*	Experiment**	Experiment	by Eq. 1	Experiment	by Eq. 1	Experiment	by Eq. 1
R.T.-373	13.63	4.22	12.4	11.43	13.8	12.88	12.3	11.72
373-473	14.81	4.07	13.4	12.30	13.9	13.91	12.6	12.50
473-573	16.19	4.23	13.4	13.40	14.7	15.10	13.3	13.41
573-673	17.56	4.38	15.0	14.49	17.2	16.29	14.9	14.31
673-773	18.94	4.54	15.8	15.58	18.0	17.49	16.4	15.22
773-873	20.31	4.70	16.5	16.67	18.0	18.68	17.3	16.13
873-973	21.69	4.86	15.8	17.77	19.7	19.87	18.8	17.04
973-1073	23.06	5.02	14.2	18.85	20.5	21.06	21.2	17.94
1073-1173	24.44	5.18	11.0	19.95	23.8	22.26	21.2	18.85
1173-1273	25.81	5.33	15.0	21.04	27.0	23.44	22.8	19.76
1273-1373	27.19	5.50	16.5	22.14	27.0	24.64	22.0	20.67

* $\alpha_m = \{12.75 + 0.01375\ (T\text{-}273)\ (K)\} \times 10^{-6}/K$

** $\alpha_f = \{3.83 + 1.584 \times 10^{-3}\ (T\text{-}273)\ (K)\} \times 10^{-6}/K$

*** α is calculated based on the mod-point of each temperature range

Levin proposed upperbound (α_U) and lowerbound(α_L) on CTE of a composite, which are given by

$$\alpha_L = \overline{\alpha E / E} < \alpha_C < \overline{\alpha K / K} = \alpha_U \qquad (1)$$

where α_C is the true CTE of the composite, K is bulk modulus, and bar on the top of symbols denotes the volume averaged quantity, for examples

$$\overline{E} = V_f E_f + V_m E_m,\ \overline{\alpha E} = V_f \alpha_f E_f + V_m \alpha_m E_m \qquad (2)$$

In the above equations, V_f and V_m are the volume fraction of fiber and matrix, respectively. The Levin's upperbound, α_U is very close to the lowerbound α_L. It was found that the Levin's lowerbounds, Eq. (1) give rise to reasonably accurate prediction for the CTE of the MMCs except for CTE O of W-ThO_2 composite at high temperatures, i.e., T > 1073 K. The stage observed in W-ThO_2 at higher temperature is mainly attributed to the plastic deformation of the matrix at these temperatures (Wakashima *et al.*, 1974). Namely, onset of the plastic deformation in the matrix phase will make the CTE of the MMC lower than the case where both the matrix and fiber undergo only elastic deformation.

Effect of Thermal Cycling.

Dimensional and Microstructural Changes. The warpage and shrinkage which were observed in W-ThO_2 composite after thermal cycling is due to the nonuniformity of tungsten fiber. As Petrasek and Signorelli (1981) have also reported, no evident debonding was observed in W-ThO_2 composite except for microcracks in the surface area. These cracks may have existed before thermal cycling, then the population and averaged size of the cracks presumably increased during the thermal cycling, resulting in the degradation of interfacial bonding. For FP alumina composite, even though no debondings were observed by SEM, degradation of the residual tensile properties occurred in 15%V_f FP alumina composite.

Tensile properties. The effect of thermal cycling on the tensile strength is shown in Figs. 11. The degradation of the strength occurred most severely in 15%V_f FP alumina composite. The severe degradation of the strength of 15%V_f FP alumina composite may be attributed to relatively large fiber aspect ratio and also to large volume fraction of fibers which are randonmly distributed. These may have caused insufficient bonding of matrix-fiber or matrix itself. On the other hand, 5%V_f FP alumina composite showed the highest strength and elongation even after thermal cycling. It is simply because adequate amount of the matrix material has penetrated into fiber network and well bonded to the fibers, thus securing the more efficient load transfer between fiber and matrix. As for W-ThO_2 composite, modest increase in the strength can be expected from low volume fraction of fiber i.e., $V_f = 0.09$. It should be noted here that the strength of unreinforced FeCrAlY matrix alone is smaller than that reported by Jackson *et al.* (1987). This poor performance in the strength of the matrix is attributed to the HIP process in our experiment. Namely the process of burning off the polymer binder used in preform fabrication was made in air at 473 K, which may have caused the formation of thin oxide layer on FeCrAlY powder.

CONCLUSION.

By this preliminary study, the effect of alumina short fiber on reducing the thermal expansion of matrix are observed to some extent but still unsatisfactory. And also 5%V_f FP alumina short fiber composite was found to have the best thermal fatigue properties among those MMCs investigated. In order to make sure the effect of fillers such as FP alumina short fiber on reducing CTE mismatch, further investigation is needed in both theoretically and experimentally.

ACKNOWLEDGEMENT

This work was supported in part by a gift from Mitsubishi Heavy Industries, Ltd. to the Department of Mechanical Engineering, University of Washington.

REFERENCES.

Armstrong, W.D. and M. Taya (1988). In: Proc. 4th U.S.-Japan Conf. on Composite Mater. in press

Bhatt, R. T., and H. H. Grimes (1983). Thermal degradation of the tensile properties of unidirectionally reinforced FP-alumina/EZ 33 magnesium composites. In:*Mechanical Behavior of Metal-Matrix Composites*, (J.E.Hack *et al.* ed.), pp.51-64. TMS-AIME, New York.

Chawla, K. K. (1976). Thermal fatigue damage in borsic Al (6061) composites. *J.Mat. Sci. Letters, 11*, 1567-1569.

Jackson, M. R. and R. L. Mehan (1987). LPPD iron base metal matrix composites. In: *Sixth International Conference of composite materials ICCM VI* (F. L. Matthews *et al.* ed.), Vol. 2, pp.2.431-2.440.

Levin, V.M, (1987), *Mechanica Tverdogo Telo*, Vo. 2, pp. 88-94.

Olsen, G. C., and S. S. Tompkins (1979). Continuous and cyclic thermal exposure induced degradation in boron reinforced 6061 aluminum composites. In: *Failure mode in Composite, Vol. IV*, pp.1-21. TMS-AIME, New York.

Park, Y. H., and H. L. Marcus (1983). Influence of interface degradation and environment on the thermal and fracture fatigue properties of titanium matrix continuous SiC fiber composite. In:*Mechanical Behavior of Metal-Matrix Composites*, (J. E. Hack *et al.* ed.), pp.65-75. TMS-AIME, New York.

Patterson, W. G. and M. Taya (1985). Thermal cycling damage of SiC whisker/2124 aluminum. In: *Fifth International Conference on Composite Materials ICCM-V* (W. C. Harrigan *et al.* ed.), pp.53-66. AIME, Pennsylvania.

Petrasek, D. W. and R. A. Signorelli (1981). Tungsten fiber reinforced super alloys-A status review. NASA TM-82590.

Yoda, S., R. Takahashi, K. Wakashima and S. Umekawa (1979). Fiber/matrix interface porosity formation in tungsten fiber/copper composites on thermal cycling. *Met. Trans. A*, 10A, pp.1976-1978.

Taya, M. and T. Mori (1987). Modeling of dimensional change in metal matrix composite subjected to thermal cycling. In: *Thermomechanical Couplings in Solids*. (H. D. Huiand and D. S. Nguyen ed.), pp.147-162. Elsevier Science Publishers, B. V., North-Holland.

Taya, M. and R. J. Arsenault (1989). In: *Metal Matrix Composites; Thermomechanical Behavior, Chapt. 4*, Pergamon Books, Ltd., in press

Wakashima, K., M. Otsuka and S. Umekawa (1974). Thermal expansion of heterogeous solids containing aligned elliposidl inclusions. *J. Com. Mater.*,Vol. 8, pp. 391-404.

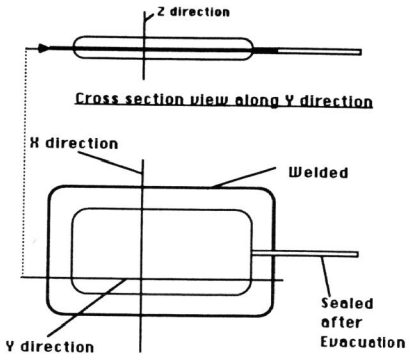

Fig 1. Schematic configuration of HIP container.

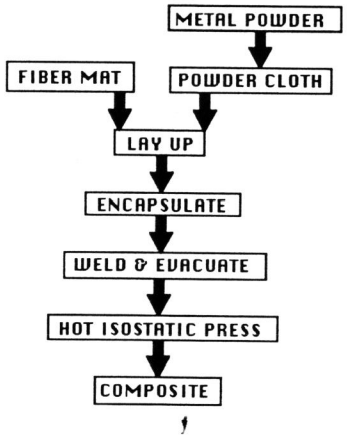

Fig. 2. Schematic diagram of composite processing.

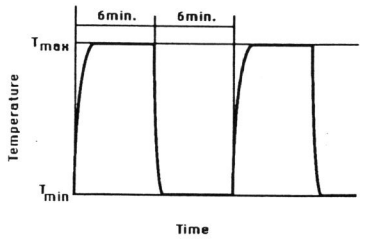

Fig. 3. Typical Temperature Time.

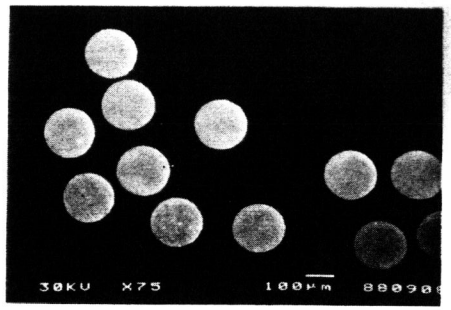

Fig. 4. Cross section micrograph of W-1%ThO_2/FeCrA1Y composite.

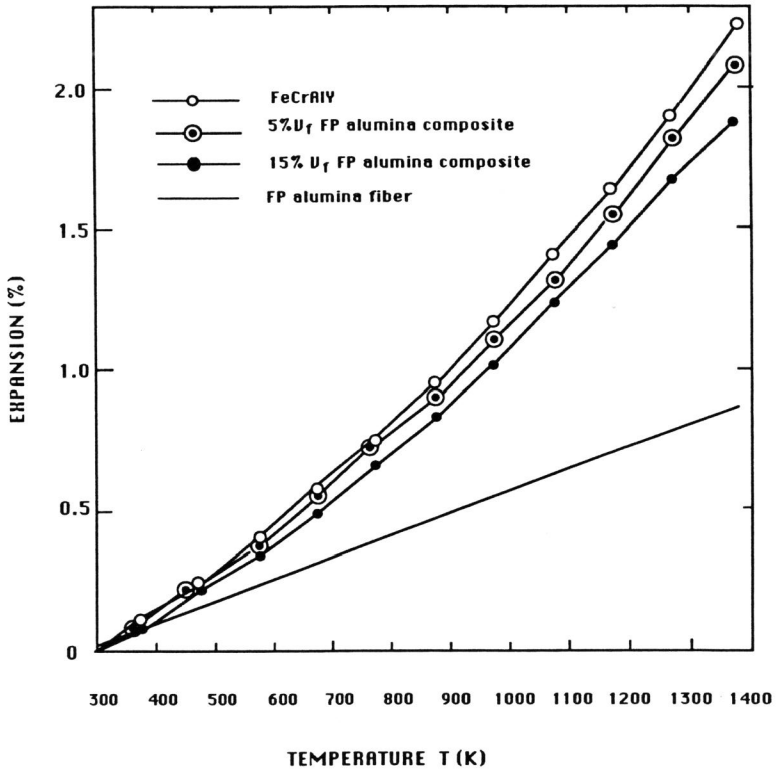

Fig. 5. Thermal expansion of FP alumina composite, FeCrA1Y matrix and FP alumina fiber.

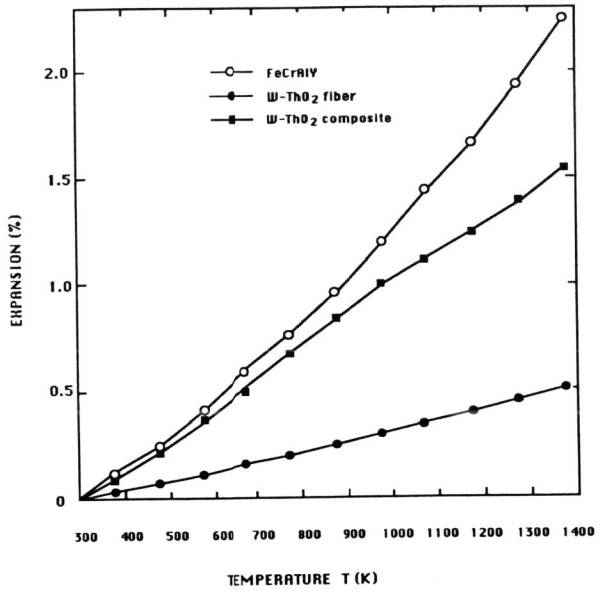

Fig. 6. Thermal expansion of W-ThO_2 composite, FeCrA1Y matrix and W-ThO_2 fiber.

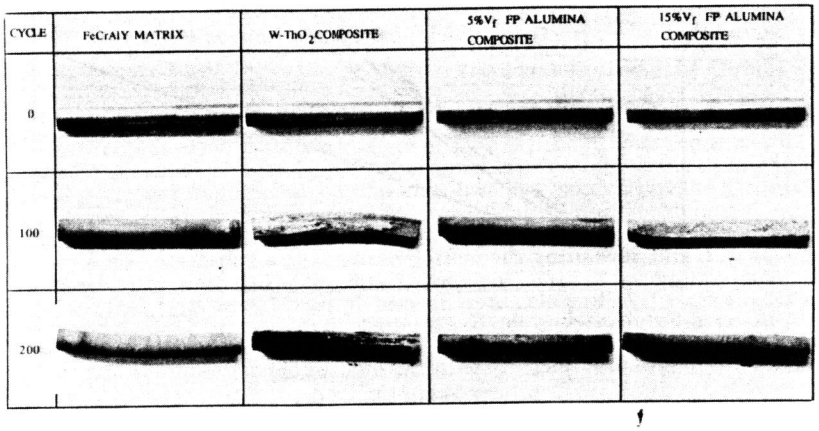

Fig. 7. The effect of thermal cycling on specimens.

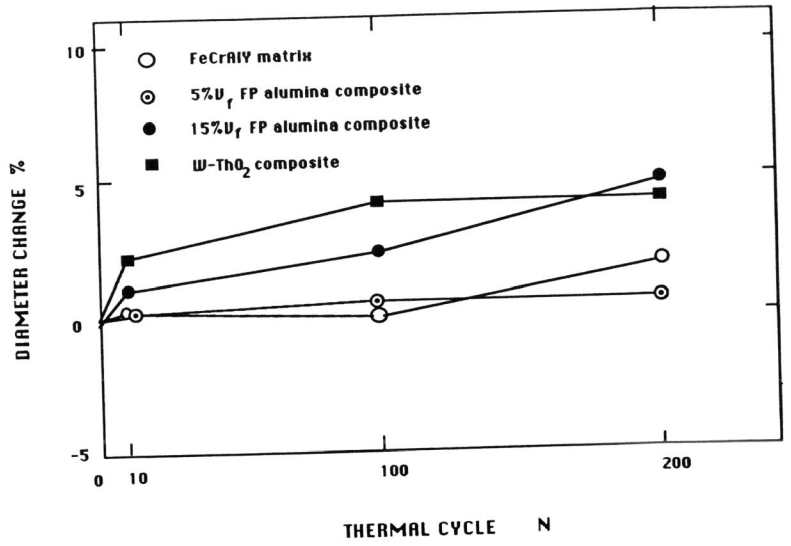

Fig. 8. Dimensional change in the diameter of MMC specimen (i.e., along the radia direction) after thermal cycling.

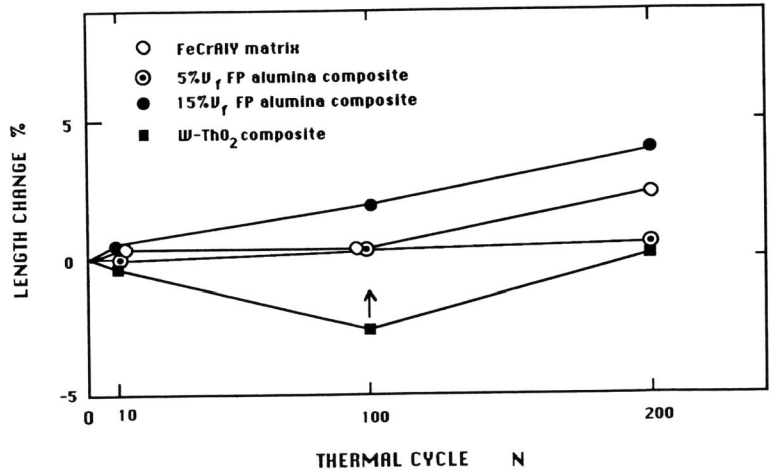

Fig. 9. Dimensional change (length) after thermal cycling.

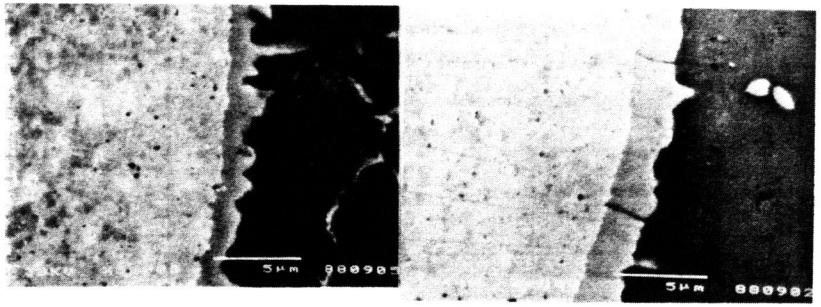

(a) (b)

Fig. 10. Microstructure of W-ThO_2 composite specimen (a) uncycled, (b) thermal cycled 200 times.

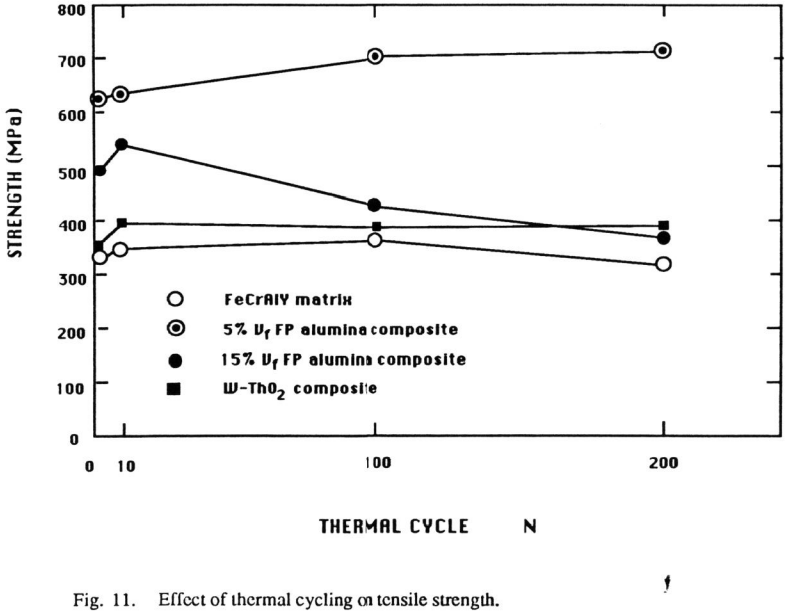

Fig. 11. Effect of thermal cycling on tensile strength.